Robust Integration of High-level Dispatchable Renewables in Power System Operation

Hongxing Ye, *Member, IEEE,* Jianhui Wang, *Senior Member, IEEE,* Yinyin Ge, *Student Member, IEEE,* Jia Li, *Student Member, IEEE,* Zuyi Li, *Senior Member, IEEE*

***Abstract*—The increasing penetration of Renewable Energy Sources (RES) requires more Flexibility Resources (FR), generally thermal units and storages, must be kept in the system to accommodate the uncertainties from RES. The challenge is how the system can survive when the RES level is very high. In this paper, RESs are considered as full-role market participants. They can bid in the day-ahead market, and the powers they deliver to the market are controllable up to their maximum available powers. Therefore, RESs are effectively dispatchable and can function as FR providers. To integrate dispatchable renewables, a two-stage robust Unit Commitment (UC) and dispatch model is established. In the first stage, a base UC and dispatch is determined. In the second stage, all FRs including RESs are used to accommodate the uncertainties, which is a Mixed-Integer Programming (MIP) problem. It is proved that the solution to the max-min problem can be identified directly whether the strong duality holds or not for the inner minimization problem. The solution robustness is guaranteed by including only one extra scenario. Numerical results show the effectiveness of the proposed model and its advantages over the traditional robust UC model with high level RES penetration.**

***Index Terms*—Dispatchable Renewable, Power System Operation, Uncertainty, Flexibility, Robust Optimization**

NOMENCLATURE

Indices

t	index of time intervals
i, l, m	index of thermal units, transmission lines, and buses
r	index of RES units
f	index of fast startup units

Functions and sets

$\mathcal{F}_1$	feasible region for base-case UC and dispatch
$\mathcal{F}_2$	feasible region for robust UC and dispatch
$\mathcal{F}_3$	feasible region for feasibility check problem
$\mathcal{F}_4$	feasible region for worst-case UC and dispatch
$\mathcal{U}$	uncertainty set
$C_f^F(\cdot)$	cost related with fast startup unit f
$C_i^I(\cdot)$	cost related to UC for thermal unit i
$C_i^P(\cdot)$	cost related to dispatch for thermal unit i
$C_r^R(\cdot)$	bid-based cost related to RES unit r
$\mathcal{G}_m$	set of thermal units located at bus m
$\mathcal{Q}_m$	set of fast startup units located at bus m
$\mathcal{R}_m$	set of RES units located at bus m

Constants

α	confidence interval parameter
β	RES energy level
N_R	number of RES units
N_T	number of time intervals
$d_{m,t}$	aggregated equivalent load at bus m time t
F_l	transmission line flow limit for line l
$\Gamma_{l,m}$	shift factor for line l with respect to bus m
$P_i^{\min}$	minimum power output for unit i
$P_i^{\max}$	maximum power output for unit i
r_i^u, r_i^d	ramping-up/down limits between sequential intervals for unit i
R_i^u, R_i^d	ramping-up/down limits for uncertainty accommodation for unit i
$u_{r,t}$	uncertainty bound of the power output for unit r at time t
$\tilde{P}_{r,t}^R$	expected power output for unit r at time t

Variables

$\epsilon_{r,t}$	power output uncertainty for unit r at time t
$\boldsymbol{\epsilon}$	a compactor vector form of all uncertainties
$\bar{P}_{r,t}$	the uncertain maximum available power output for unit r at time t
$I_{i,t}$	on/off status indicator for unit i at time t
$x_{i,t}^{\text{on}}, x_{i,t}^{\text{off}}$	number of hours unit i has been on/off at time t
$y_{i,t}, z_{i,t}$	start-up/shut-down indicators for unit i at time t
$P_{i,t}$	generation dispatch for unit i at time t
$\hat{P}_{i,t}$	re-dispatch for unit i at time t when uncertainty is revealed
$I_{f,t}^F$	on/off status indicator for unit f at time t when uncertainty is revealed
$P_{f,t}^F$	dispatch of unit f at time t when uncertainty is revealed
$P_{r,t}^R$	delivered power for unit r at time t
$\hat{P}_{r,t}^R$	re-dispatched power of unit r at time t
$P_{m,t}^{\text{inj}}$	net power injection at bus m time t
$\hat{P}_{m,t}^{\text{inj}}$	net power injection at bus m time t after re-dispatch
$s_{m,t}$	slack variable at bus m time t

H. Ye is with Cleveland State University, Cleveland, OH 44114, USA. J. Wang is with Argonne National Lab, Argonne, IL 60439, USA. Y. Ge and are Z. Li with Illinois Institute of Technology, Chicago, IL 60616, USA. J. Li is with Tsinghua University, Beijing, 10084, China. (e-mail: hye9@hawk.iit.edu; jianhui.wang@anl.gov; yge9@hawk.iit.edu; Jia.Li@iit.edu; lizu@iit.edu.)

I. INTRODUCTION

The variable Renewable Energy Sources (RES) are dramatically increasing in recent years. They produce competitive energy that is low in production cost and free of carbon emission. However, the power output from RES such as wind and solar is intermittent and volatile. They also introduce more uncertainties into the system operation and electric markets. In

the U.S. Day-ahead Market (DAM), the new uncertainties due to the integration of variable RES are mainly from the forecasting errors of the available RES power next day. The Unit Commitment (UC) and Economic Dispatch (ED) problems in DAM rely on the accurate system data forecasting for the next day. The uncertainties from RESs pose new challenges for the UC and ED problems in DAM, which have attracted extensive attentions in recent years [1]–[6].

The UC and ED problem is a daily task for the Independent System Operators (ISO) and Regional Transmission Organization (RTO) [7]–[10]. In the UC problem, the on/off schedule of each generating unit, also called Unit Commitment (UC), in the next day is determined. The objective is to find the least cost UC combinations and power output levels for all the units to supply the load while respecting the system-wide constraints as well as unit-wise constraints. The system-wide constraints may include the load demand balance, transmission capacity limit, and reserve requirement. The unit-wise constraints are normally composed of generation capacity limits, ramping rate limits, and minimum on/off time limits [9]–[11].

To accommodate the uncertainties from variable RES, both scenario-based stochastic optimization and robust optimization are studied extensively for the UC problems [3]–[5], [12]–[16]. The main idea of the scenario-based stochastic UC is to generate a large number of sample points for the random variables (i.e. uncertainties), then reduce the sample set to a much smaller one, which can be modeled and solved by modern Mixed-Integer Programming (MIP) solvers. In general, there are three main drawbacks of the scenario-based stochastic UC. The first one is that scenario generation is not easy due to the absence of the Probability Distribution Function (PDF) in Monte Carlo based approaches or the large computation burden in Numerical Weather Predication (NWP) based approaches [17]. The second one is that the scenario reduction may cause uncertainty survivability issue of the system in some cases. The third one is that it is computationally intractable in general unless heuristic solution techniques are used. Therefore, researchers in [4], [5] introduce the two-stage Robust UC (RUC) to overcome first two drawbacks. In the traditional two-stage RUC, the UC solution is determined in the first stage, which leads to the least cost in the worst case. The ED is considered in the second stage, and it can be adjusted to accommodate any uncertainty in a pre-determined set. Because of the robustness associated with the solution, the two-stage RUC becomes another research focus in recent years. However, as the worst case is optimized, it has the issue of the over-conservativeness. In order to get an economical effective solution, authors in [14] introduce a unified approach to combine the scenario-based stochastic UC and RUC. [18] also introduce a new concept, the recourse cost requirement, to optimize the base case. Both the scenario-based stochastic UC and robust UC are computation intensive. Researchers in [13] reported the Column and Constraint Generation (CG) algorithm to accelerate the RUC solution approach. On the other side, Affine Policy (AP) [19] is introduced to simplify the recourse actions in the robust approaches [15], [16], [20]. With strong assumptions, the intractable robust problem is converted to a convex and tractable one in the AP approach. However, the price of using AP is the reduction of the recourse actions, which often leads to non-zero optimality gap.

In most of the existing approaches, all the RES outputs (or uncertainties) must be accommodated. When the penetration level is low, RES generally can lower the total operation cost. However, it may not be true when the RES penetration level is high and the system has to accommodate all available energy from RES. A fundamental reason is that deliverable ramping capabilities must be kept in the system to accommodate the uncertainties. These ramping capabilities, also called flexibilities or reserves, are expensive when the uncertainty level is high.

A potential solution to this problem is to make RES dispatchable. That is, the RES power delivered to the system is controllable from zero to the maximum available power. As presented in [21], the wind power output could be controlled with the latest technologies. It is also possible to control the output of photovoltaic (PV) array by adjusting the array angle. On the other hand, too much zero-cost generation from RES could depress the Locational Marginal Price (LMP) at the injection point to a very low level or even zero or negative, which would ultimately affect the profit of RES. Thus, rather than acting as price takers, RESs could bid into the electricity markets as dispatchable resources. Recently, some researchers have explored the dispatchability of wind power [22], [23]. When RES is controllable in RUC, authors in [23] show that the strong duality can help to reformulate the second-stage problem. At the same time, if RES is dispatchable, it is also possible for RES units to provide reserves [24]–[26]

In this paper, we focus on the variable RESs, such as wind and solar. They are modeled as dispatchable resources with bid offers. The RES unit cannot be modeled as the traditional unit as the maximum available RES power output is a random variable. A two-stage adaptive RUC is formulated. In the first stage, a set of RUC and ED solution is obtained, which optimally determines the least cost flexibility (or reserves) in the system. In the second stage, these flexibilities can accommodate any uncertainties within the confidence interval. The flexibility includes fast startup units, thermal units with available ramping capabilities, and dispatchable RESs. Different from [24], we will analyze and investigate the dispatchable resources from the perspective of the system operator. The main contributions of this paper are

1) A novel robust integration model of high-level dispatchable RESs is proposed. Fast startup units are considered in the second stage of RUC, which involves integer variables. It is proved that the solution to the non-convex max-min problem in the second stage can be obtained directly. Different from [23], the conclusion holds even without the strong duality of the inner-level minimization problem.
2) A fast solution approach is presented to solve the proposed RUC. Only two scenarios need to be considered. One is the base-case scenario and the other is the worst-case scenario. The robustness is guaranteed by modeling the worst-case scenario. The computational challenge in existing RUC is addressed by solving a converted single-level MIP problem with dispatchable RES.

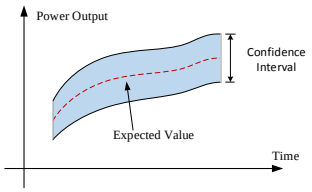

Fig. 1. The confidence interval and the expected value of RES power output

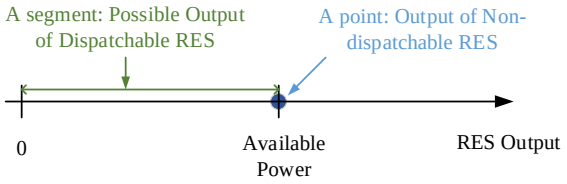

Fig. 2. The actual RES output delivered to the grid

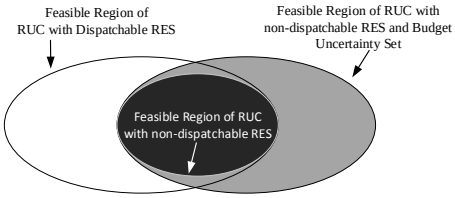

Fig. 3. Feasible region comparison for RUC

3) It is revealed that the dispatchable RESs are more economical in terms of total system cost in the RUC. The bid offers of the RESs are modeled. The cost for accommodating all power from RESs is high when the uncertainty is large. With high level penetration, dispatching the RESs is potentially a new direction in the electricity markets.

The rest of this paper is organized as follows. In Section II, the new robust integration model for dispatchable RES is presented. Then, a solution approach is presented in Section III. Case studies are presented in Section IV. Finally, Section V concludes this paper.

II. Robust Integration of Dispatchable RES

In the propose model, the RESs are treated as market participants with full roles. They are different from the traditional RUC [4], [5], [18], [27], where power outputs of variable RESs are considered as negative loads, and the bids of these power outputs are zeros. In this paper, the RESs can bid, and the output $P^R_{r,t}$ of RES unit r at time t is a decision variable. Due to the forecast errors, the maximum available power output $\bar{P}^R_{r,t}$ is an uncertain parameter.

$$\bar{P}^R_{r,t} = \tilde{P}^R_{r,t} + \epsilon_{r,t}, \forall r, t, \tag{1}$$

where $\tilde{P}^R_{r,t}$ is the expected power output for RES unit r at t, and $\epsilon_{r,t}$ is the uncertainty. The uncertainty set $\mathcal{U}$ is defined as

$$\mathcal{U} := \{\boldsymbol{\epsilon} \in \mathbb{R}^{N_R N_T} : -u_{r,t} \le \epsilon_{r,t} \le u_{r,t}, \forall r, t\}. \tag{2}$$

Fig. 1 illustrates the possible RES power output. The uncertainty always falls within the confidence interval defined by $u_{r,t}$. The expected RES output is not modeled as the inelastic negative load anymore [18]. Instead, it is set as the upper bound of $P^R_{r,t}$ in the first stage

$$0 \le P^R_{r,t} \le \tilde{P}^R_{r,t}, \forall r, t. \tag{3}$$

In this paper, only intervals of the uncertainty are considered, which is similar to the interval optimization [28]. However, in the interval approach, the largest power flows in all lines are considered simultaneously, which requires corresponding transmission capacities be reserved simultaneously. This is not only conservative but also hardly true as it is very difficult if not impossible to find an uncertainty point leading to the largest power flows in all lines simultaneously. The proposed model does not have this issue. Hence, it is less conservative than the interval approach. The budget constraint in some robust approaches [5] is ignored. At the first glance, the uncertainty set in this paper is larger than that in other models, which may lead to the issue of over-conservativeness. However, the dispatchability of RESs reduces the conservativeness, especially when the RES penetration level is high. As shown in Fig. 2, power output of RES is inelastic in traditional robust approaches, and it is a point. When the RES is dispatchable, the RES power delivered to the grid is within a segment. Therefore, the feasible region of the re-dispatch problem is increased. Fig. 3 compares the feasible regions for different RUC models. In robust approaches with non-dispatchable RES, adding the budget parameter (i.e. reducing the uncertainty set) can enlarge the feasible region. In comparison, dispatching RES also enlarges the feasible region.

The new RUC can be formulated as

$$\text{(P1):} \quad \min \quad \left\{ \begin{aligned} &\sum_i \sum_t \left(C^P_i(P_{i,t}) + C^I_i(I_{i,t}) \right) \\ &+ \sum_r \sum_t C^R_r(P^R_{i,t}) \end{aligned} \right\} \tag{4}$$

$$\text{s.t.} \quad \left\{ P_{i,t}, I_{i,t}, P^R_{i,t} \right\} \in \mathcal{F}_1 \cap \mathcal{F}_2 \tag{5}$$

where $\mathcal{F}_1$ is the feasible region for the base case in the first stage, and $\mathcal{F}_2$ guarantees the existence of the re-dispatch when the uncertainty is revealed in the second stage. The objective function (4) is to minimize the base cost. The solution to (P1) must be robust against any realization of the uncertainty in the second stage. $\mathcal{F}_1$ is defined as

$$\mathcal{F}_1 := \Big\{ (P, I, P^R) : \sum_i P_{i,t} + \sum_r P^R_{r,t} = \sum_m d_{m,t}, \forall t \tag{6}$$

$$P^{\text{inj}}_{m,t} = \sum_{i \in \mathcal{G}_m} P_{i,t} + \sum_{r \in \mathcal{R}_m} P^R_{r,t} - d_{m,t}, \forall m, t \tag{7}$$

$$-F_l \le \sum_m \Gamma_{l,m} P^{\text{inj}}_{m,t} \le F_l, \forall l, t \tag{8}$$

$$I_{i,t} P^{\min}_i \le P_{i,t} \le I_{i,t} P^{\max}_i, \forall i, t \tag{9}$$

$$P_{i,t} - P_{i,(t-1)} \le r^u_i (1 - y_{i,t}) + P^{\min}_i y_{i,t}, \forall i, t \tag{10}$$

$$-P_{i,t} + P_{i,(t-1)} \le r^d_i (1 - z_{i,t}) + P^{\min}_i z_{i,t}, \forall i, t \tag{11}$$

$$(x^{\text{on}}_{i,t-1} - T^{\text{on}}_i)(I_{i,t-1} - I_{i,t}) \ge 0, \forall i, t \tag{12}$$

$$(x^{\text{off}}_{i,t-1} - T^{\text{off}}_i)(I_{i,t} - I_{i,t-1}) \geq 0, \forall i, t \tag{13}$$

$$0 \leq P^R_{r,t} \leq \tilde{P}^R_{r,t}, \forall r, t \Big\} \tag{14}$$

Equation (6) stands for the load balance constraint, where $d_{m,t}$ is the load demand at bus m at time t. The net power injection is modeled in (7), where $\mathcal{G}_m$ and $\mathcal{R}_m$ denote the thermal unit set and RES unit set at bus m, respectively. The network constraints are enforced in (8). Equation (9) model the upper and lower power output limits of the thermal units. The thermal units are enforced by the sequential ramping rate limits in (10)-(11), where $I_{i,t}$, $y_{i,t}$, and $z_{i,t}$ are the indicators of the unit being on, started-up, and shut-down, respectively. Equations (10) and (11) show that a unit has to operate at its minimum capacity in two cases: right after it is turned on or right before it is turned off, which implies that the unit cannot provide reserve in those two cases. The minimum on/off time constraints are modeled in (12)-(13). The dispatchable RES output respects the constraint (14). The ramping rates of the RES output are not modeled in this paper. If the ramping constraints of RES similar to those of thermal units are enforced for RES, all the conclusions in this paper are still valid.

The feasible region $\mathcal{F}_2$ in (5) is defined as

$$\mathcal{F}_2 := \Big\{(P, I, P^R) : \forall \boldsymbol{\epsilon} \in \mathcal{U}, \exists \{\hat{P}_{i,t}, P^F_{i,t}, \hat{P}^R_{i,t}\} \text{ such that}$$

$$\sum_i \hat{P}_{i,t} + \sum_r \hat{P}^R_{r,t} + \sum_f P^F_{f,t} = \sum_m d_{m,t}, \forall t \tag{15}$$

$$\hat{P}^{\text{inj}}_{m,t} = \sum_{i \in \mathcal{G}_m} \hat{P}_{i,t} + \sum_{r \in \mathcal{R}_m} \hat{P}^R_{r,t} + \sum_{f \in \mathcal{Q}_m} P^F_{f,t} - d_{m,t}, \forall m, t \tag{16}$$

$$-F_l \leq \sum_m \Gamma_{l,m} \hat{P}^{\text{inj}}_{m,t} \leq F_l, \forall l, t. \tag{17}$$

$$I_{i,t} P^{\min}_i \leq \hat{P}_{i,t} \leq I_{i,t} P^{\max}_i, \forall i, t \tag{18}$$

$$-I_{i,t} R^d_i \leq \hat{P}_{i,t} - P_{i,t} \leq I_{i,t} R^u_i, \forall i, t \tag{19}$$

$$I^F_{f,t} P^{\min,F}_f \leq P^F_{f,t} \leq I_{f,t} P^{\max,F}_f, \forall f, t \tag{20}$$

$$0 \leq \hat{P}^R_{r,t} \leq \tilde{P}^R_{r,t} + \epsilon_{r,t}, \forall r, t \Big\}. \tag{21}$$

where $\hat{P}_{i,t}$ and $\hat{P}^R_{i,t}$ are the re-dispatches of thermal units and RES units, respectively, when the uncertainties are revealed. (15)-(16) are the load balance constraint, net power injection, and network constraints, respectively, after the uncertainty is revealed. The re-dispatch of thermal unit is limited by the ramping rate in (19). The $P^F_{f,t}$ denotes the power output of the fast startup units. It is enforced by the upper and lower generation limit in (20), where $I^F_{f,t}$ is the on/off indicator. The RES power level is not greater than the available maximum output in (21). It is noted that the ramping limit between $\hat{P}_{i,t}$ and $\hat{P}_{i,t+1}$ is not modeled. Instead, we model the ramping constraints from $P_{i,t}$ to $P_{i,t+1}$, from $P_{i,t}$ to $\hat{P}_{i,t}$, and from $P_{i,t+1}$ to $\hat{P}_{i,t+1}$. In the DAM, it is assumed that the operator has enough time to adjust the dispatches.

An advantage of the model formulated in this paper is that the deliverable ramping capability is guaranteed at each time interval. It becomes useful when considering the causality of the economic dispatch. In the existing two-stage robust approach, the causality is ignored. In comparison with the multi-stage robust approaches [20], the full recourse actions instead of AP policies are modeled in this paper which leads to more optimistic solution. It should be noted that the ramping constraint in this paper is less precise as ramping constraint between $\hat{P}_{i,t}$ and $\hat{P}_{i,t+1}$ is relaxed. This is consistent with the industry practice which is also called "corrective" dispatch after contingencies occur. It is worth mentioning that the solution approach in the next section is still applicable when the ramping constraint between $\hat{P}_{i,t}$ and $\hat{P}_{i,t+1}$ is enforced.

III. Solution Approach

In this section, we show that the two-stage RUC model (P1) can be converted into a single-level MIP problem. Accordingly, the solution to the original two-stage RUC problem can be obtained by solving the converted single-level MIP without using the Bender's decomposition or the Column Generation (CG) framework [4], [5], [13]. To solve (P1), a feasibility check problem regarding $\mathcal{F}_2$ is established as

$$\text{(FC)} \max_{\boldsymbol{\epsilon} \in \mathcal{U}} \min_{(\hat{P}, \hat{P}^R, P^F, s) \in \mathcal{F}_3(P, I, P^R, \boldsymbol{\epsilon})} \sum_t \sum_m s_{m,t}, \tag{22}$$

where $\mathcal{F}_3(P, I, P^R, \boldsymbol{\epsilon})$ is defined as

$$\mathcal{F}_3(P, I, P^R, \boldsymbol{\epsilon}) := \Big\{(\hat{P}, \hat{P}^R, P^F, s) :$$

$$\sum_i \hat{P}_{i,t} + \sum_r \hat{P}^R_{r,t} + \sum_f P^F_{f,t} = \sum_m d_{m,t} - s_{m,t}, \forall t \tag{23}$$

$$-F_l \leq \sum_m \Gamma_{l,m} (\hat{P}^{\text{inj}}_{m,t} + s_{m,t}) \leq F_l, \forall l, t \tag{24}$$

$$0 \leq \hat{P}^R_{r,t} \leq \tilde{P}^R_{r,t} + \epsilon_{r,t}, \forall r, t \tag{25}$$

$$s_{m,t} \geq 0, \forall m, t \tag{26}$$

$$(16), (18), (19), (20) \Big\}.$$

It is observed that the problem (FC) is a two-level problem. The outer-level maximization problem is to find out the worst $\boldsymbol{\epsilon}$ which leads to the largest load curtailment (i.e. summation of $s_{m,t}$). The inner-level minimization problem is to find out the re-dispatch solution which leads to the lowest load curtailment. In comparison to the model shown in [18], no traditional generation curtailment (i.e. slack variable) is formulated. The reason is that the output of the dispatchable RES can be reduced and no over generation occurs. The relation between the problem (FC) and feasible region $\mathcal{F}_2$ can be described by the following proposition.

Proposition 1. $\{P_{i,t}, I_{i,t}, P^R_{r,t}\} \in \mathcal{F}_2$, if and only if the optimal value to the max-min problem (FC) is zero.

To solve the problem (FC), the inner problem is normally converted to its dual problem in literatures [4], [5], [18], where a bilinear problem is therefore formulated. In this paper, since the fast startup units are modeled in the re-dispatch process, the strong duality does not hold. Therefore, the traditional approach cannot be applied. Fortunately, the optimal solution to (FC) can be identified by the following theorem.

Theorem 1. The optimal solution to (FC) is obtained when $\epsilon_{r,t} = -u_{r,t}, \forall r, t$.

Proof. Denote the solution to (FC) as $\{\boldsymbol{\epsilon}^* : \epsilon^*_{r,t} = -u_{r,t}\}$, $z(P, I, P^R, \boldsymbol{\epsilon}^*)$ stands for the optimal value to the inner MIP problem when $\boldsymbol{\epsilon} = \boldsymbol{\epsilon}^*$. Assume there exists a point $\boldsymbol{\epsilon}' \neq \boldsymbol{\epsilon}^*$ where $\epsilon_{r',t} > -u_{r',t}$ for RES r', the optimal value $z(P, I, P^R, \boldsymbol{\epsilon}') > z(P, I, P^R, \boldsymbol{\epsilon}^*)$. According to (25),

$$\{\hat{P}_{r',t} : 0 \leq \hat{P}^R_{r',t} \leq \tilde{P}^R_{r',t} - u_{r',t}\} \subset \{\hat{P}_{r',t} : 0 \leq \hat{P}^R_{r',t} \leq \tilde{P}^R_{r',t} + \epsilon_{r',t}\}.$$

As other constraints remain the same,

$$\mathcal{F}_3(P, I, P^R, \boldsymbol{\epsilon}^*) \subseteq \mathcal{F}_3(P, I, P^R, \boldsymbol{\epsilon}') \tag{27}$$

holds. The feasible region is enlarged, then the optimal values to the inner minimization problem have following relation

$$z(P, I, P^R, \boldsymbol{\epsilon}') \leq z(P, I, P^R, \boldsymbol{\epsilon}^*). \tag{28}$$

It can be observed that it is contradicted with the assumption. Hence, $\boldsymbol{\epsilon}^*$ is the optimal solution to (FC), which leads to the largest load curtailment. □

The implication of Theorem 1 is that the worst case is fixed and is independent of the first stage solution $\{P_{i,t}, I_{i,t}, P^R_{r,t}\}$. Therefore, we can directly add the worst case into the RUC without solving the computation intensive max-min problem. Define

$$\mathcal{F}_4 := \Big\{(P, I, P^R, \hat{P}, \hat{P}^R, P^F) : 0 \leq \hat{P}^R_{r,t} \leq \tilde{P}^R_{r,t} - u_{r,t} \quad (15), (16), (17), (18), (19), (20)\Big\}.$$

Then the two-stage RUC (P1) is converted into a single-level MIP problem as follows.

$$\text{(P2):} \quad \min \quad \left\{ \begin{array}{l} \sum_i \sum_t \Big(C^P_i(P_{i,t}) + C^I_i(I_{i,t})\Big) \\ + \sum_r \sum_t C^R_r(P^R_{i,t}) \end{array} \right\}$$

$$\text{s.t.} \quad \Big\{P_{i,t}, I_{i,t}, P^R_{i,t}\Big\} \in \mathcal{F}_1,$$

$$\Big\{P_{i,t}, I_{i,t}, P^R_{i,t}, \hat{P}_{i,t}, \hat{P}^R_{i,t}, P^F_{f,t}\Big\} \in \mathcal{F}_4$$

If the cost of the worst case is considered similar to [14], then the new problem can be formulated as

$$\text{(P3):} \ \min \quad (1-w) \left\{ \begin{array}{l} \sum_i \sum_t \Big(C^P_i(P_{i,t}) + C^I_i(I_{i,t})\Big) \\ + \sum_r \sum_t C^R_r(P^R_{i,t}) \end{array} \right\}$$

$$+ w \left\{ \begin{array}{l} \sum_i \sum_t \Big(C^P_i(\hat{P}_{i,t}) + C^I_i(I_{i,t})\Big) \\ + \sum_r \sum_t C^R_r(\hat{P}^R_{i,t}) + \sum_f \sum_t C^f_f(P^F_{f,t}) \end{array} \right\}$$

$$\text{s.t.} \quad \Big\{P_{i,t}, I_{i,t}, P^R_{i,t}\Big\} \in \mathcal{F}_1,$$

$$\Big\{P_{i,t}, I_{i,t}, P^R_{i,t}, \hat{P}_{i,t}, \hat{P}^R_{i,t}, P^F_{f,t}\Big\} \in \mathcal{F}_4.$$

In comparison to the CG based framework, the main difference is that only one additional scenario is considered, which guarantees the robustness (i.e. system can survive when the uncertainty is revealed without load curtailment). Therefore, the increased computation burden due to the robustness is acceptable.

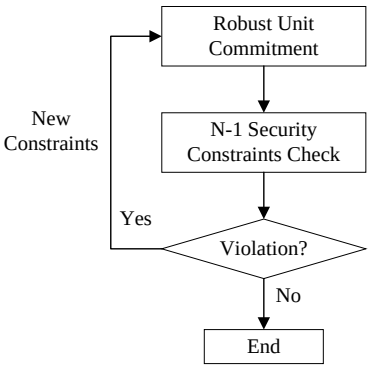

Fig. 4. Flowchart of incorporating the security constraints. $N-1$ security constraints are checked at the current solution to RUC, and violated constraints are added.

As the RESs are dispatchable, they can also be used to accommodate the uncertainties. Hence, RESs do not require FRs any more, they actually function as FRs. This is especially critical for systems with high level RESs.

A. Incorporation of Security Constraints

ISO and RTO often add the security constraints in the UC problems in case of line or generator contingencies [8], [9], [11], [29]. The new problem incorporated with these constraints is called security-constrained unit commitment (SCUC) problem. The security constraints can also be incorporated in the proposed models. When a generator is out of service, its output must be zero. When a line is out of service, we will have different shift factors in network constraints (8) and (17). The general principles of the model and solution approach still apply.

The main challenge of adding security constraints is the large number of the constraints. Consider a system with L lines and T periods. The number of the $N-1$ network security constraint is $2 \times (L-1) \times L \times T$. In practice, even the modern MIP solvers are unable to handle the model if all these constraints are added directly. Our approach in this paper is to only add the potentially active security constraints. The flowchart in Fig. 4 illustrates how the $N-1$ security constraints are incorporated in the RUC model. After solving the RUC, the security constraints are checked and only the violated constraints are added back to the RUC model. A similar approach is also widely applied in the literature and in the industry to address the computational challenge due to the security constraints [9], [30].

IV. Case Study

The proposed RUC model and solution approaches are tested with the modified IEEE 118-bus system. The system is consisted of 54 thermal units, 186 branches, 15 wind farms, and 15 solar farms. The MIP solver Gurobi 5.6.3 [31] is utilized to solve the MIP problems on PC with Intel i7-3770@3.40GHz 8GB RAM.

The peak load is 6600MW in 24 hours for the modified IEEE 118-bus system. Hour 11 and Hour 20 are two peak

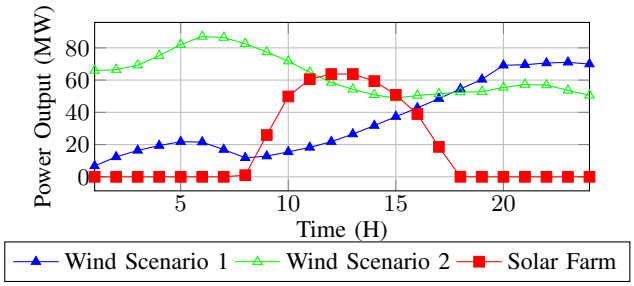

Fig. 5. Aggregated Wind and Solar Power Output Forecasting

TABLE I
THE BASE CASE COST AND AVERAGE COST COMPARISON WITH INCREASING RES OUTPUTS (SCENARIO 1)

β	Base Cost ($)		Average Cost ($)		UCs (h)	
	Dis.	Non-Dis.	Dis.	Non-Dis.	Dis.	Non-Dis.
1.0	1,613,353	1,613,397	1,570,180	1,570,617	625	641
1.6	1,415,987	1,419,017	1,380,330	1,381,957	629	642
1.7	1,386,416	1,400,034	1,351,274	1,363,356	644	704
2.2	1,253,351	infeasible	1,212,849	infeasible	658	infeasible
5.0	697,865	infeasible	663,279	infeasible	388	infeasible

points. Both the solar farms and the wind farms are simulated simultaneously in this section. The aggregated wind power output forecast is obtained from ISO-NE. The data in scenario 1 and scenario 2 is one fifth of the day-ahead forecasts for wind power output on 06-17-2015 and 03-31-2015, respectively. The solar farm output is from NREL. The aggregated solar power is the output from Arizona on 01-01-2006. The 15 wind farms and 15 solar farms are located at 30 different buses. The detailed data including generating unit parameters, line reactance and ratings, and load profiles can be found at http://motor.ece.iit.edu/Data/ROUC_118.xls.

The curves in Figure 5 depict the expected value of the output $\tilde{P}^R_{r,t}$. The actual available RES power is $\tilde{P}^R_{r,t} + \epsilon_{r,t}$. In this section, the uncertainty $\epsilon_{r,t}$ is assumed within the confidence interval, i.e. $-\alpha\tilde{P}^R_{r,t} \leq \epsilon_{r,t} \leq \alpha\tilde{P}^R_{r,t}$. $\alpha \in \mathbb{R}$ is chosen from 20% to 30% in the simulations. Denote β as the RES level. $\beta = 1$ stands for the base RES level.

A. Dispatchable RES V.S. Non-Dispatchable RES

In many robust literatures, the generation outputs from RES are modeled as inelastic load [4], [5], [15], [16]. Any fluctuation from RES output must be accommodated with flexible resources. In contrast, the RESs are assumed to be dispatchable within their available power level in this paper. In this part, the main objective is to compare the impacts of the RES dispatches. For simplicity, the fast startup units are not considered in the second stage, which may cause computation issue for the traditional RUC. At the same time, the bids of the RESs are assume to be zeros. The confidence interval is set to 25%, and $w = 0$.

The simulations are performed in two steps. In the first step, the Robust UC and Dispatch are determined based on (P2) or other robust approaches with non-dispatchable RESs [4], [5], [18]. In the second step, 1000 samples of $\boldsymbol{\epsilon}$ are generated for the RESs following the normal distribution. Then the available flexibilities are re-dispatched with the realized RES outputs. We perform the sensitivity analysis with the RESs output level in terms of operation cost and UC hours.

Table I presents the base cost and average cost comparisons between solutions with dispatchable and non-dispatchable RESs with wind scenario 1. The "base cost" is the total operation cost to supply the load with the expected RES output levels. The "average cost" is the average total operation costs for all the sample points. Column "β" shows the increasing RES level. The total expected available power from wind and solar is 19,197 MWh, which is 14.6% of the total load demand 131,472MWh. When β reaches 5, the available power from wind and solar is 73% of the total load demand. It can be observed that the cost for the RUC with dispatchable RES in this paper is always smaller than the one with non-dispatchable RES. It is also consistent with the feasible region comparison shown in Figure 3. With smaller feasible unit dispatch region, the traditional RUC normally is more conservative. The total UC hours ("UCs(h") represents the total committed hours for all units. In order to provide more flexible resources, the traditional RUC with non-dispatchable RESs has to keep more units ON. In comparison, the total UC hours of the approach in this paper are always smaller.

An important observation is that the cost differences change with the RES production levels. For the base level (i.e. $\beta = 1$), the base-case cost difference is \$1,613,397 - \$1,613,353 = \$ 44, and the average cost difference is \$1,570,617 - \$1,570,180 = \$437. When the RES production level increases to 1.7, the solution with dispatchable RES can save \$1,400,034 - \$1,386,416=\$13,618 in base-case cost in comparison to the one with non-dispatchable RES. The average cost saving increases to \$1,351,274 - \$1,363,356=\$12,082 from \$437. It demonstrate that the proposed approach with dispatchable RES leads much lower cost when the RES level is high.

Another observation is that the RUC with non-dispatchable RES becomes infeasible when the RES production level increases to 2.2. It is assumed that the confidence interval $\epsilon_{r,t}$ is [-25%, 0.25%] of the available production level. Hence, with larger expected power output, the uncertainties the system should accommodate also increase. However, the ramping capability, which is provided by the thermal unit, has an upper limit. When the uncertainty is above the limit, no feasible solution can be found for the RUC with non-dispatchable RES. The system operators may have to curtail the load or shut down thermal units regardless of the UC schedules. In contrast, the problem with dispatchable RES is feasible even when the RES level reaches 5.0. The reason is that the RESs can also provide flexibilities. At a level of 5.0, the total average cost is reduced to \$663,279, which is 42.24% of the base-case average cost \$1,570,180.

Table II shows another set of cost results with wind scenario 2 depicted Figure 5. The total expected available RES production is 22.3% of the load demand. It can be observed that when RES level is over 1.2, the RUC with non-dispatchable RES becomes infeasible. When the RES level increases to

TABLE II
THE BASE-CASE COST AND AVERAGE COST COMPARISON WITH INCREASING RES OUTPUTS (SCENARIO 2)

β	Base Cost ($)		Average Cost ($)		UCs (h)	
	Disp.	Non-Disp.	Disp.	Non-Disp.	Disp.	Non-Disp.
1.0	1,446,969	1,447,583	1,410,778	1,411,577	614	631
1.2	1,352,607	1,357,410	1,317,716	1,322,519	606	638
1.3	1,308,989	infeasible	1,274,367	infeasible	592	infeasible
5.0	351,987	infeasible	324,916	infeasible	248	infeasible

TABLE III
PROCURED RES ENERGY WITH INCREASING RES LEVELS AND DECREASING RES BIDS ($\alpha = 25\%, w = 0$)

Bid[a]	$\beta = 1.0$			$\beta = 2.0$			$\beta = 5.0$		
	RES[b]	(%)	UCs[c]	RES	(%)	UCs (h)	RES	(%)	UCs
5	29,321	100.00	614	53,908	91.93	554	103,824	70.82	213
0	29,321	100.00	614	54,542	93.01	635	104,364	71.19	248
-5	29,321	100.00	614	54,583	93.08	640	105,270	71.81	304

[a] $/MWh; [b] MWh; [c] h

5.0, the total expected available RES power is 111.5% of the load demand. There are only 248 UC hours in this case and the total cost drops to $324,916. Although the RES power is larger than the load demand, two factors prevent the cost from being zero. One is that there are no energy storages to store the over-generated power. For example, wind power reaches its peak point while the load demand is lower at 6:00AM. The other one is the line congestions, which also prevent free RES energy from all being delivered to certain load buses.

B. Impacts of the RES Bids

In the DAM, the energies are traded at the financially binding prices between market participants. In this part, the bids of the RES are simulated to show differences of the energy settlements. The simulations are analyzed and discussed from RES energy accommodation point of view rather than the market cost perspective. Hence, three different simple bid offers (i.e. $5/MW, $0/MW, and $-5/MW) are simulated, and the typical wind scenario 2 is used. As an example of negative bidding price, the ISO New England allows the market participants to bid at negative prices since December 3, 2014. Four groups of sensitivity analysis for RES procurement are discussed in this part:

- with increasing RES levels;
- with increasing uncertainty levels;
- with increasing weight factor of the worst case;
- with increasing fast startup units.

1) Increasing RES Levels: The procured RES energy and UC hours With increasing RES level are presented in Table III. The RES levels are chosen as 1.0, 2.0, and 5.0. The procured RES energy in DAM are shown in the columns denoted as "RES". They are the same with different bid offers when the production level β=1. However, if the RES increases to 2.0 times of the base level, then different bid offers result in different procured RES energy. Column "%" shows the procured RES energy as a percentage of the expected available RES energy. For example, the procured RES energy is 53,908 MWh with a $5/MWh bid offer, which is 91.93% of the expected available RES energy. In contrast, if the bid offer decreases to $0/MWh, then the procured RES energy increases by 54,542 MWh - 53,908 MWh = 634 MWh. In other words, the thermal units supply 634 MWh fewer load demands. Table III also shows that the UC hours increase to 635 from 554 in this case. An interesting observation is that fewer thermal units are committed to supply more loads when the bid offer changes from $0/MWh to $5/MWh. The reason is that, to accommodate more cheaper $0/MWh RES energy, more generation reserves must be kept in order to accommodate the uncertainties. Thus, more units are committed, which can provide more ramping capabilities. It indicates that the opportunity cost of keeping these reserves is smaller than that of curtailing the RES energies. A similar trend can also be observed when β=5.0.

TABLE IV
PROCURED RES ENERGY WITH INCREASING UNCERTAINTY LEVELS AND DECREASING RES BIDS ($\beta = 2.0, w = 0$)

Bid[a]	α=0%			α=20%			α=30%		
	RES[b]	(%)	UCs[c]	RES	(%)	UCs	RES	(%)	UCs
5	57,867	98.68	388	55,524	94.68	457	52,071	88.79	633
0	57,909	98.75	388	56,423	96.22	565	52,293	89.17	661
-5	57,971	98.86	388	56,626	96.56	589	52,390	89.34	674

[a] $/MWh; [b] MWh; [c] h.

With increasing β, the procured percentage of expected available RES energy is decreasing. For example, when $\beta = 1$, all RES energy is procured in DAM. In contrast, when $\beta = 5.0$, only around 71% of the available RES energy is scheduled to be delivered into the system. It indicates that when the RES level is high, the most economical way is to have some RES energy spilled. It becomes expensive to accommodate all the RESs as the reserve cost is high at this time. It is worth mentioning that the total operation cost is negative when β=5.0 and the bid offer is $-5/MWh.

2) Increasing Uncertainty Levels: As mentioned above, more generation reserves are required if more energy from uncertain RESs are delivered into the grid. In this paragraph, we discuss the impacts of the uncertainty levels on RES energy procurement in DAM. Table IV presents the procured RES energy in DAM with different bid offers and uncertainty levels. It is assumed that the RES level $\beta = 2.0$, which is about 44.6% of the total load demand. It can be observed with the same bid offer, the increase of the uncertainty level causes the drop of the amount of procured RES energy. For example, with $0/MWh bid offer, the procured RES energy is 56,423 MWh, and total UC hours are 565 when $\alpha = 20\%$. When α increases to 30%, then the procured RES energy drops to 52,293 MWh, and the total UC hours increase to 661. Similar trends are also observed when the bid offer is $5/MWh or $-5/MWh. In general, more uncertainties are accommodated by more ramping capabilities in the system.

Another observation is that with the increasing uncertainty,

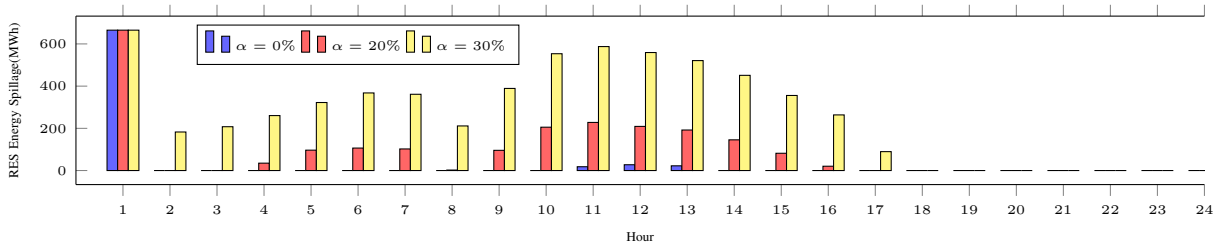

Fig. 6. RES Energy Spillage w.r.t. Different Uncertainty Level ($\beta = 2.0, w = 0$, bid=\$0/MWh).

TABLE V
PROCURED RES ENERGY WITH INCREASING WEIGHT FACTORS FOR THE WORST-CASE COST AND DECREASING RES BIDS ($\alpha = 25\%, \beta = 2.0$)

Bid [a]	$w = 0$			$w = 0.2$			$w = 1$		
	RES [b]	(%)	UCs [c]	RES	(%)	UCs	RES	(%)	UCs
5	53,908	91.93	554	53,399	91.06	481	47,010	80.16	421
0	54,542	93.01	635	54,040	92.15	562	47,010	80.16	421
-5	54,583	93.08	640	54,542	93.01	623	47,010	80.16	421

[a] \$/MWh; [b] MWh; [c] h.

TABLE VI
PROCURED RES ENERGY WITH INCREASING NUMBER OF FAST STARTUP UNITS AND DECREASING RES BIDS ($\alpha = 25\%, \beta = 2.0, w = 0.2$)

Bid [a]	# of FU=0			# FU=3			# FU=6		
	RES [b]	(%)	UCs [c]	RES	(%)	UCs	RES	(%)	UCs
5	53,399	91.06	481	56,918	97.06	411	57,799	98.56	394
0	54,040	92.15	562	57,018	97.23	416	57,804	98.57	394
-5	54,542	93.01	623	57,427	97.93	465	57,842	98.64	393

[a] \$/MWh; [b] MWh; [c] h.

the procured RES energy percentage (%) is decreasing. A higher uncertainty level requires more spinning reserves in the system to ensure the solution robustness. With the assumption $\alpha = 0\%$, there are no uncertainties for the RES energy. The procured RES energy percentage is 98.75% with zero bid offer. When the uncertainty level $\alpha = 30\%$, the procured percentage drops by 9.58% to 89.17%. It indicates that compared with the cost of the supporting reserve for RES energy, it is much cheaper to schedule the thermal units to supply the load. In Figure 6, the spillage of the RES energy is depicted. It shows that the RES energy spillages occur from 1:00AM to 17:00AM. At Hour 1, the ON/OFF statuses of many units are changed from those at Hour 0. With the assumption that the spinning reserve is zero when the unit is at its first ON hour or the last OFF hour, the reserves provided at Hour 1 is small. Consequently, the spillage is the largest at Hour 1.

3) Increasing Weight Factors for the Worst-Case Cost: In Table III and Table IV, the weight factor for the worst-case cost is set to 0. In this part, we perform the sensitivity analysis of RES energy procurement with the increasing weight factors for the worst-case cost. The simulation results are presented in Table V. In general, the increase of the weight factor results in fewer RES energy procurements. When $w = 0$, only the base case is considered. For example, with bid offer at \$5/MWh, the procured RES energy percentage decreases from 91.93% to 80.16% when w is changed from 0 to 1. In the extreme case $w = 1$, only the worst case is optimized. No upward supporting reserves for RES energy are needed in this case. Therefore, we have fewer UC hours. Consequently, the system can accommodate fewer RES energies in the base case. Similar trends can also be observed when the bid offers are \$0/MWh and \$-5/MWh.

4) Increasing Fast Startup Units: When considering the fast startup units, the system has more flexible resources, although the price of these resources is expensive. In Table VI, the RES energy procured in the DAM is presented with the increasing number of fast startup units. It can be observed that the increase of the fast startup units leads to more RES energy procurements. For example, the procured RES energy percentage increases to 98.57% from 91.06% with \$5/MWh bid offer when the number of fast startup units changes to 6 from 0. On the other hand, the UC hours are decreasing. It indicates that more flexible resources help the system accommodate more RES energies.

TABLE VII
THE BASE-CASE COST AND PROCURED ENERGY COMPARISON

β	RUC W/O Security Cons.			RUC W/ Security Cons.		
	Base Cost (\$)	RES [a]	(%)	Base Cost (\$)	RES	(%)
1	1,446,969	29,321	100	1,460,505	29,321	100
2	1,054,580	54,542	93.01	1060365	54,386	92.74
3	762,672	74,196	84.35	768,703	73,937	84.05

[a] MWh.

C. Impact of Security Constraint

Table VII presents a comparison of the base-case cost and procured RES energy between the models with and without $N - 1$ security constraints. In general, the incorporation of security constraints increases the base-case cost in the RUC models. For example, when $\beta = 1$, the base-case cost is increased by $\$13,536 = 1,460,505 - 1,446,969$ although the procured RES amounts are both 23,321MWh. In some cases, the incorporation of security constraints also results in the reduction of the procured RES. For instance, when $\beta = 2$, the percentage of procured RES energy is reduced to 92.74% from 93.01% if security constraints are added in the model.

Table VIII presents the procured RES energy amounts and UC hours with increasing RES levels when the security constraints are enforced. Table VIII reveals a similar relation between procured RES energy, RES level, and bid as discussed in Section IV-B-1 for Table III, where the security constraints

TABLE VIII
PROCURED RES ENERGY WITH INCREASING RES LEVELS AND SECURITY CONSTRAINTS ($\alpha = 25\%, w = 0$)

Bid[a]	$\beta = 1.0$			$\beta = 2.0$			$\beta = 5.0$		
	RES[b]	(%)	UCs[c]	RES	(%)	UCs (h)	RES	(%)	UCs
5	29,321	100	668	53,952	92	574	102,589	69.98	261
0	29,321	100	668	54,386	92.74	626	102,990	70.25	285
-5	29,321	100	668	54,454	92.86	634	103,696	70.73	329

[a] \$/MWh; [b] MWh; [c] h

are not enforced. The main difference is that the procured RES energy in the RUC model with security constraints is less than that without security constraints. The decrement of RES integration is also consistent with the analysis for Table VII.

These simulations verify that the security constraints can be incorporated in the proposed RUC model. The results show that the security constraints reduce the feasible region of the UC problem. The results also indicate that while security constraints can enhance the reliability, they also have adverse impacts on the economic efficiency and RES integration.

D. Computation Comparison

The robustness of the approach in this paper can be guaranteed by an extra scenario (i.e. the worst case). With the default parameters, the MIP solver can get the solution within 2 seconds for the IEEE 118-Bus system. The existing RUC with non-dispatchable RES normally costs more time to get the solution. Without any acceleration techniques, approaches in [4], [5], [13] cannot get the solution in 2 hours. Two factors slow down the solution process in the these approaches. The first one is that these algorithms often involve iterative processes. For example, in the Benders Decomposition approach [4], [5], [27], a large number of new MIP problems with Benders cuts generated by solving subproblems must be solved repeatedly. In the Column Generation approach [13], [18], different worst points are calculated each time. Several increasing-size MIP problems need to be solved repeatedly in the iterative process. The second one is that solving the non-convex max-min subproblem is a challenging task. In the approach proposed in this paper, no max-min subproblem needs to be solved.

V. CONCLUSIONS

In this paper, a robust UC and dispatch model considering the RES bids are proposed in the system with high RES level. It is proved that with the dispatchable RES, the worst case for the second stage can be directly identified. The conclusion always holds whether the strong duality holds for the re-dispatch problem or not. With this conclusion, the robustness can be guaranteed by adding only one extra scenario in the original UC problem.

The simulation results in this paper show that by increasing the RES level, the total cost can be lowered. However, there is an increasing chance that the traditional robust UC with non-dispatchable RES is infeasible if the RES level is high. The simulation results also show that it is not the most economic strategy to accommodate all the power from RESs into the grid. By taking the advantage of the dispatchable RES, this paper shows that the RES can also provide flexibilities. In the future power system with high RES penetration, the dispatchability of the RES will play a crucial role. It is a promising and attractive new research topic.

In the current market, only conventional units are allowed to provide the reserves. That is because the most important task of the ancillary products (i.e. reserves) is to maintain the reliability of the system. In order to become a reserve provider, RES owners still need to address other challenges, such as reliability and power quality. From the market participant's point of view, investigating the optimal bidding strategy is an interesting research topic if RES is allowed to participate in future reserve market. The profit of RES is highly related to the pricing mechanism within the robust optimization framework. We have done some work on this topic [32], where the RES is non-dispatchable. The general principles in [32] also apply when the RES is dispatchable.

When UC is fixed, the Lagrangian multipliers for (3) can serve as the reserve price, which is also the opportunity cost [8]. If the reserve is defined as

$$\tilde{P}^R_{r,t} - P^{R^*}_{r,t}$$

the optimal dispatch $P^{R^*}_{r,t}$, the energy price LMP, and the reserve price constitute the partial competitive equilibrium [33]. In other words, if the RES units are considered as price takers, they can get the maximum profits by following the ISO's instruction $P^{R^*}_{r,t}$. However, the reserve the RES provides may not be equal to

$$\tilde{P}^R_{r,t} - P^{R^*}_{r,t},$$

as $\tilde{P}^R_{r,t}$ is only the expected power output not the actual power output.

$$\tilde{P}^R_{r,t} - P^{R^*}_{r,t} - u_{r,t}$$

is a more reliable value for reserve.

REFERENCES

[1] "Integration of wind into system dispatch," New York ISO, Tech. Rep., 2008.

[2] "Integration of renewable resources," California ISO, Tech. Rep., 2010. [Online]. Available: http://www.casio.com

[3] L. Wu, M. Shahidehpour, and T. Li, "Stochastic security-constrained unit commitment," *IEEE Trans. Power Syst.*, vol. 22, no. 2, pp. 800–811, 2007.

[4] R. Jiang, J. Wang, and Y. Guan, "Robust unit commitment with wind power and pumped storage hydro," *IEEE Trans. Power Syst.*, vol. 27, no. 2, pp. 800 – 810, 2012.

[5] D. Bertsimas, E. Litvinov, X. Sun, J. Zhao, and T. Zheng, "Adaptive robust optimization for the security constrained unit commitment problem," *IEEE Trans. Power Syst.*, vol. 28, no. 1, pp. 52–63, 2013.

[6] R. Wiser and M. Bolinger, "2011 wind technologies market report," Lawrence Berkeley National Laboratory, Tech. Rep., 2012.

[7] X. Guan, P. B. Luh, H. Yan, and J. Amalfi, "An optimization-based method for unit commitment," *Int. J. Electr. Power & Energy Syst.*, vol. 14, no. 1, pp. 9–17, 1992.

[8] *ISO New England Manual for Market Operations Manual M-11 Revision 44*, ISO New England Inc., access:May 19, 2015. [Online]. Available: http://www.iso-ne.com/static-assets/documents/rules_proceds/isone_mnls/M11/m_11_market_operations_revision_44_05_23_13.doc

[9] M. Shahidehpour, H. Yamin, and Z. Li, *Market Operations in Electric Power Systems: Forecasting, Scheduling, and Risk Management*, 1st ed. Wiley-IEEE Press, 2002.

[10] H. Wu, X. Guan, Q. Zhai, and H. Ye, "A systematic method for constructing feasible solution to SCUC problem with analytical feasibility conditions," *IEEE Trans. Power Syst.*, vol. 27, no. 1, pp. 526–534, 2012.

[11] Z. Li and M. Shahidehpour, "Security-constrained unit commitment for simultaneous clearing of energy and ancillary services markets," *IEEE Trans. Power Syst.*, vol. 20, no. 2, pp. 1079–1088, 2005.

[12] S. Takriti, J. Birge, and E. Long, "A stochastic model for the unit commitment problem," *IEEE Trans. Power Syst.*, vol. 11, no. 3, pp. 1497–1508, 1996.

[13] B. Zeng and L. Zhao, "Solving two-stage robust optimization problems using a column-and-constraint generation method," *Operations Research Letters*, vol. 41, no. 5, pp. 457–461, sep 2013.

[14] C. Zhao and Y. Guan, "Unified stochastic and robust unit commitment," *IEEE Trans. Power Syst.*, vol. 28, no. 3, pp. 3353–3361, 2013.

[15] J. Warrington, P. Goulart, S. Mariethoz, and M. Morari, "Policy-based reserves for power systems," *IEEE Trans. Power Syst.*, vol. 28, no. 4, pp. 4427–4437, 2013.

[16] R. A. Jabr, "Adjustable robust OPF with renewable energy sources," *IEEE Trans. Power Syst.*, vol. 28, no. 4, pp. 4742–4751, 2013.

[17] E. M. Constantinescu, V. M. Zavala, M. Rocklin, S. Lee, and M. Anitescu, "A computational framework for uncertainty quantification and stochastic optimization in unit commitment with wind power generation," *IEEE Trans. Power Syst.*, vol. 26, no. 1, pp. 431–441, Feb 2011.

[18] H. Ye and Z. Li, "Robust security-constrained unit commitment and dispatch with recourse cost requirement," *IEEE Trans. Power Syst.*, DOI: 10.1109/TPWRS.2015.2493162 (early access).

[19] A. Ben-Tal, A. Goryashko, E. Guslitzer, and A. Nemirovski, "Adjustable robust solutions of uncertain linear programs," *Math. Program., Ser. A*, vol. 99, no. 2, pp. 351–376, Mar. 2004.

[20] A. Lorca, A. Sun, E. Litvinov, and T. Zheng, "Multistage adaptive robust optimization for the unit commitment problem," *Operations Research*, vol. 64, no. 1, pp. 32–51, 2016.

[21] E. D. Castronuovo, J. Martínez-Crespo, and J. Usaola, "Optimal controllability of wind generators in a delegated dispatch," *Electric power systems research*, vol. 77, no. 10, pp. 1442–1448, 2007.

[22] B. Hu, L. Wu, and M. Marwali, "On the robust solution to scuc with load and wind uncertainty correlations," *IEEE Trans. Power Syst.*, vol. 29, no. 6, pp. 2952–2964, 2014.

[23] G. Morales-Espaa, M. Davidson, L. Ramrez-Elizondo, , and M. M. de Weerdt, "Robust unit commitment with dispatchable wind: An lp reformulation of the second stage." [Online]. Available: http://www.optimization-online.org/DB_HTML/2014/09/4542.html

[24] J. Liang, S. Grijalva, and R. G. Harley, "Increased wind revenue and system security by trading wind power in energy and regulation reserve markets," *IEEE Transactions on Sustainable Energy*, vol. 2, no. 3, pp. 340–347, July 2011.

[25] M. Hedayati-Mehdiabadi, J. Zhang, and K. W. Hedman, "Wind power dispatch margin for flexible energy and reserve scheduling with increased wind generation," *IEEE Transactions on Sustainable Energy*, vol. 6, no. 4, pp. 1543–1552, Oct 2015.

[26] T. Soares, P. Pinson, T. V. Jensen, and H. Morais, "Optimal offering strategies for wind power in energy and primary reserve markets," *IEEE Trans. Sustain. Energy*, vol. 7, no. 3, pp. 1036–1045, July 2016.

[27] R. Jiang, M. Zhang, G. Li, and Y. Guan, "Two-stage network constrained robust unit commitment problem," *J. Eur. Oper. Res.*, vol. 234, no. 3, pp. 751 – 762, 2014.

[28] Y. Wang, Q. Xia, and C. Kang, "Unit commitment with volatile node injections by using interval optimization," *IEEE Trans. Power Syst.*, vol. 26, no. 3, p. 17051713, 2011.

[29] Y. Fu, Z. Li, and L. Wu, "Modeling and solution of the large-scale security-constrained unit commitment," *IEEE Trans. Power Syst.*, vol. 28, no. 4, pp. 3524–3533, Nov 2013.

[30] Y. Chen, A. Casto, F. Wang, Q. Wang, X. Wang, and J. Wan, "Improving large scale day-ahead security constrained unit commitment performance," *IEEE Trans. Power Syst.*, vol. PP, no. 99, pp. 1–12, 2016.

[31] I. Gurobi Optimization, *Gurobi Optimizer Reference Manual*, 2014. [Online]. Available: http://www.gurobi.com

[32] H. Ye, Y. Ge, M. Shahidehpour, and Z. Li, "Uncertainty marginal price, transmission reserve, and day-ahead market clearing with robust unit commitment," *IEEE Trans. Power Syst.*, DOI:10.1109/TPWRS.2016.2595621, (early access).

[33] A. Mas-Colell, M. D. Whinston, J. R. Green *et al.*, *Microeconomic theory*. Oxford university press New York, 1995, vol. 1.

Hongxing Ye (S'14-m'16) received his B.S. degree in Information Engineering, in 2007, and M.S. degree in Systems Engineering, in 2011, both from Xi'an Jiaotong University, China, and the Ph.D. degree in Electrical Engineering from the Illinois Institute of Technology, Chicago in 2016. He is currently an Assistant Professor in the Department of Electrical Engineering and Computer Science at Cleveland State University. His research interests include large-scale optimization in power systems, electricity market, renewable integration, and cyber-physical system security in smart grid. He is "Outstanding Reviewer" for IEEE Transactions on Power Systems and IEEE Transactions on Sustainable Energy in 2015. He received Sigma Xi Research Excellence Award at Illinois Institute of Technology in 2016.

Jianhui Wang (M'07-SM'12) received the Ph.D. degree in electrical engineering from Illinois Institute of Technology, Chicago, IL, USA, in 2007. Presently, he is the Section Lead for Advanced Power Grid Modeling at the Energy Systems Division at Argonne National Laboratory, Argonne, IL, USA. Dr. Wang is the secretary of the IEEE Power & Energy Society (PES) Power System Operations Committee. He is an associate editor of Journal of Energy Engineering and an editorial board member of Applied Energy. He is also an affiliate professor at Auburn University and an adjunct professor at University of Notre Dame. He has held visiting positions in Europe, Australia and Hong Kong including a VELUX Visiting Professorship at the Technical University of Denmark (DTU). Dr. Wang is the Editor-in-Chief of the IEEE Transactions on Smart Grid and an IEEE PES Distinguished Lecturer. He is also the recipient of the IEEE PES Power System Operation Committee Prize Paper Award in 2015.

Yinyin Ge (S'14) received her B.S. degree and M.S. degree from Xi'an Jiaotong University, China in 2008 and 2011, both in electrical engineering. She is currently a Ph.D. candidate of Electrical Engineering at the Illinois Institute of Technology, Chicago. Her research interests are power system optimization and modeling, Smart Grid and power system stability and control.

Jia Li (S'15) received the B.S. degree in electrical engineering from Tsinghua University, Beijing, China, in 2012. He is currently pursuing the Ph.D. degree at the Department of Electrical Engineering, Tsinghua University. His current research interests include power system optimization under uncertainty.

Zuyi Li (SM'09) received the B.S. degree from Shanghai Jiaotong University, Shanghai, China, in 1995, the M.S. degree from Tsinghua University, Beijing, China, in 1998, and the Ph.D. degree from the Illinois Institute of Technology (IIT), Chicago, in 2002, all in electrical engineering. Presently, he is a Professor in the Electrical and Computer Engineering Department at IIT. His research interests include economic and secure operation of electric power systems, cyber security in smart grid, renewable energy integration, electric demand management of data centers, and power system protection.